Discrete-lattice theory for Frenkel-defect aggregation in irradiated ionic solids

V. N. Kuzovkov*

Institute of Solid State Physics, University of Latvia, 8 Kengaraga Street, LV-1063, Riga, Latvia
and Institut für Physikalische und Theoretische Chemie, Technische Universität Braunschweig, D-38106 Braunschweig, Germany

E. A. Kotomin

Institute of Solid State Physics, University of Latvia, 8 Kengaraga Street, LV-1063, Riga, Latvia
and Fachbereich Physik, Freie Universität Berlin, 14195 Berlin, Germany

W. von Niessen

Institut für Physikalische und Theoretische Chemie, Technische Universität Braunschweig, D-38106 Braunschweig, Germany

A microscopic theory of diffusion-controlled aggregation of radiation Frenkel defects—called in ionic solids H and F centers—is presented. This is based on a discrete-lattice formalism for the single defect densities (concentrations) and the coupled joint densities of similar and dissimilar defects treated in terms of a modified Kirkwood superposition approximation. The kinetics of defect aggregation is studied in detail; the cooperative character of this process for both types of complementary defects is shown. The theory is applied to the description of the kinetics of metal colloid formation during heating of electron-irradiated CaF_2 crystals. [S0163-1829(98)06937-9]

I. INTRODUCTION

It is well known that the primary radiation defects in ionic solids—the F centers (electron trapped by anion vacancy) and the H centers (interstitial halide atoms)—begin to aggregate under intensive irradiation and at sufficiently high temperatures. This leads to the formation of alkali metal colloids and gas bubbles, respectively (see Ref. 1 and references therein); a similar process occurs also in heavily irradiated metals.[2] Intensive experimental studies of the conditions for the defect aggregation and subsequent colloid formation (such as the temperature interval, dose rate, etc.) continue nowadays for many alkali halides,[3,4] in particular for the technologically important CaF_2,[5,6] and for ceramic materials.[7] This problem is also interesting from a fundamental point of view, being an example of *pattern formation* and *self-organization* in reaction-diffusion systems far from equilibrium.[8] It should be stressed that metal colloid formation is a rather slow process which in real experiments often lasts several weeks or longer; another reason why this problem is a difficult one for direct computer (Monte Carlo) simulations is that the mobilities of the two kinds of defects involved (interstitials and vacancies) differ typically by 10–15 orders of magnitude. In order to model the F center aggregation, one has to use a very small time increment which is dictated by the highly mobile H centers.

Existing theories of radiation-induced defect aggregation and colloid formation can be classified, in terms of the mathematical formalism used, into three categories: macroscopic,[9] mesoscopic,[10,11] and microscopic.[12–15] We call *microscopic* a theory on an atomic scale which uses no fitting or uncertain parameters like numerous reaction rates but only several basic defect parameters such as the diffusion energies and interaction energies. Such a theory has been presented recently by us.[12] However, the continuum approxi-

mation used there has led to nonphysical problems associated with cutting off the interaction potentials at the nearest-neighbor (NN) distance, and with large gradients of the correlation functions at these distances. The first point makes results very sensitive to the manner in which the potentials are defined at distances shorter than NN. The second one forces us to use very small coordinate increments in the calculations which then strongly restricts the time interval which can realistically be reached using such an approach.

In this paper we develop a microscopic, *discrete-lattice* theory of diffusion-controlled aggregation occuring during the bimolecular annihilation, $A + B \rightarrow 0$, under a permanent particle source. The theory is based on the mathematical formalism for stochastic processes in spatially extended systems which has been developed by the authors for catalytic surface reactions.[15,16] In this paper our microscopic formalism is generalized for the bulk processes in three dimensions, taking also into account creation of Frenkel defects under irradiation. To make the problem solvable, we restrict ourselves to lattice models where both elementary events (diffusion hops, recombination) and particle interactions occur only between NN particles. This is a good approximation for diffusion. However, dissimilar particle recombination in some cases, e.g., in metals, needs incorporation of longer distances. The same is true for a description of realistic long-range particle interaction, since in fact in this paper we neglect the ''tail'' of the elastic attraction of Frenkel defects which decays as r^{-3}, with r the distance between the two defects. Such approximations are unavoidable in a study of many-particle systems with a strong interaction between particles (defects).

We apply the theory to the study of the cooperative kinetics of colloid formation under irradiation of CaF_2 crystals. However, after minor modifications it can be used for other systems too, e.g., metals or microelectronic materials.

The plan of the paper is as follows: in Sec. II a physical model is described and its mathematical realization is discussed in detail in Sec. III. Section IV deals with the description of the transition rates of the basic processes and particle interactions, whereas the master equations are analyzed in Sec. V. The theory is illustrated in Sec. VI by application to H and F center aggregation kinetics in CaF_2 crystals. This effect is important for CaF_2 applications in optical windows and nanolithography. Conclusions are given in Sec. VII.

II. A PHYSICAL MODEL

The *physical model* includes creation of interstitials, i.e., H centers, and vacancies, i.e., F centers (called hereafter just defects or particles A and B). This takes place with a given (dose) rate p, AB pairs are not spatially correlated at birth and recombine when they approach each other during their migration to within the NN distance. Therefore, their macroscopic concentrations always coincide, $n = n_A = n_B$. Isolated (single) defects hop with the activation energy E_λ and are characterized by the diffusion coefficients $D_\lambda = d_\lambda \exp(-E_\lambda/k_B T)$, $\lambda = A, B$. When several defects are close together, the hop rate of a given defect to the nearest empty lattice site is determined by both the local defect configuration and the interaction between defects; this can change its *effective* diffusion coefficient D_λ^{eff} by many orders of magnitude compared to that for a single defect. This affects the *effective reaction rate K* of the A and B recombination; for the dilute system in the continuum approximation this rate is well known to be $K_0 = 4\pi r_0(D_A + D_B)$, where r_0 is the recombination radius.

From previous theoretical studies[10–12] it follows that defect attraction plays a decisive role in the aggregation process. It is incorporated in our model via three types of NN attractions between the two types of NN defects (in the spirit of the Ising model): E_{AA}, E_{AB}, and E_{BB}. Note that only a few theoretical studies have been devoted up to now to the effects of particle interaction (especially, for similar particles) in the kinetics of the bimolecular diffusion-controlled reaction $A + B \rightarrow 0$, with the emphasis on fluctuation phenomena. Rare exceptions are the papers.[17,18] Particle interactions render the kinetic equations essentially nonlinear and this causes manifestation of self-organization (pattern formation) under irradiation.

III. A MATHEMATICAL MODEL

A. Definitions

Each lattice site is given a lattice vector $\mathbf{r}_l$ and coordination number z. The state of the site $\mathbf{r}_l$ is described by the local variable σ_l. The spectrum of its values $\sigma_l = 0, A, B$ describes three possible states of the lattice site: 0 represents a vacant site, whereas A and B are sites occupied by an A or B particle, respectively. A particle aggregate or colloid is treated as a dynamical domain containing particles of one type only (A or B). In other words, an isolated particle A or particle A inside the aggregate are described in a similar way through the local state variable σ_l.

B. State probabilities

The lattice processes under consideration can be treated as stochastic Markov processes. Each lattice state characterized by a set of local variables $\boldsymbol{\sigma} = \{\sigma_1, \sigma_2, \dots\}$ arises with the probability $\rho(\boldsymbol{\sigma})$. The latter gives formally a complete probabilistic description of the system, however the equation determining $\rho(\boldsymbol{\sigma})$ cannot be solved exactly. The probabilistic description of the lattice states can be done also using another set of quantities, the so-called *many-point probabilities* which depend on i lattice sites and are coupled through recurrence sum rules. Such a limited set of probabilities better suits our particular problem.

1. Single-point probabilities

The single-point probability $\rho^{(1)}(\sigma_l)$ is the probability to find at time t the lattice site $\mathbf{r}_l$ in the state σ_l. Due to the translational invariance these probabilities can depend only on time. Using the abbreviation $\lambda = \sigma_l$, $C_\lambda = \rho^{(1)}(\sigma_l)$ one can write down the obvious normalization condition

$$\sum_\lambda C_\lambda = C_A + C_B + C_0 = 1. \tag{1}$$

In terms of physics the quantity C_λ is nothing but a simple density of particles on the lattice (site population). C_A, C_B, and C_0 are densities for particles A, B or empty sites, respectively. The usual, dimensional densities n_λ (per unit volume) are just

$$n_\lambda = \frac{C_\lambda}{a_0^3}, \tag{2}$$

where a_0 is a lattice parameter. Obviously, the use of such macroscopic values as the simple particle densities C_λ is not sufficient for the description of the particle aggregation. The latter needs a detailed analysis of the relative distribution of several types of particles on the lattice and an analysis of their relevant spatial correlations. For this purpose the two-point densities and relevant correlation functions are well suited.

2. The correlation functions

The two-point probability $\rho^{(2)}(\sigma_l, \sigma_m)$ is the probability of finding at the time t the site $\mathbf{r}_l$ in the state $\lambda = \sigma_l$ and the site $\mathbf{r}_m$ in the state $\mu = \sigma_m$. It can be formally presented in the factorized form

$$\rho^{(2)}(\sigma_l, \sigma_m) = C_\lambda C_\mu F_{\lambda\mu}(\mathbf{r}), \quad \mathbf{r} = \mathbf{r}_l - \mathbf{r}_m, \tag{3}$$

where $F_{\lambda\mu}(\mathbf{r})$ is the joint correlation function. As follows from Eq. (3), due to the translational invariance, both the two-point density and the correlation function depend only on the relative distance between two sites, $\mathbf{r}_l$ and $\mathbf{r}_m$, characterized by a vector $\mathbf{r}$. Besides, $F_{\lambda\mu}(\mathbf{r})$ satisfies several general conditions. The first one is that the correlation disappears at large distances (due to the short-range nature of the spatial correlations). This means that as $r \rightarrow \infty$, the states of sites $\mathbf{r}_l$ and $\mathbf{r}_m$ are statistically independent which results in $\rho^{(2)}(\sigma_l, \sigma_m) = \rho^{(1)}(\sigma_l)\rho^{(1)}(\sigma_m)$, i.e.,

$$\lim_{r \to \infty} F_{\lambda\mu}(\mathbf{r}) = 1. \tag{4}$$

The second condition is a relation between single- and two-point densities, the sum rule

$$\sum_{\sigma_m} \rho^{(2)}(\sigma_l, \sigma_m) = \rho^{(1)}(\sigma_l), \tag{5}$$

or

$$\sum_{\mu} c_{\mu}^{(\lambda)}(\mathbf{r}) = 1, \quad c_{\mu}^{(\lambda)}(\mathbf{r}) = C_{\mu} F_{\lambda\mu}(\mathbf{r}). \tag{6}$$

The latter equation is similar to Eq. (1) and permits also a similar interpretation. The quantity

$$c_{\mu}^{(\lambda)}(\mathbf{r}) = \rho^{(2)}(\sigma_l, \sigma_m)/\rho^{(1)}(\sigma_l) \tag{7}$$

defines the conditional probability that the site at $\mathbf{r}$ is in the state μ when the central site $\mathbf{r}_l$ is in the state λ.

3. Density of single particles

To handle the complicated statistical problem under question, we use a reduced probabilistic description of the many-particle system in terms of single and joint particle densities only, i.e., many-point probabilities $\rho^{(k)}$ are expressed through simple densities (concentrations) C_{λ} and the joint correlation functions $F_{\lambda\mu}(\mathbf{r})$. Let us illustrate this principle by an example. We call an *isolated particle* (single center) a local state where the site $\mathbf{r}_l$ is in the state $\lambda = \sigma_l$, whereas all its nearest-neighbor (NN) sites are empty ($\{\sigma\}_l^z = \{\sigma_1, \ldots, \sigma_z\} = \{0, \ldots, 0\}$). The probability to find an isolated (single) particle C_{λ}^s is defined by the $(z+1)$-point probability $C_{\lambda}^s = \rho^{(z+1)}$. The density of dimer-, trimer- and higher particle configurations can be found in a similar way (see below), i.e., through many-particle densities with a larger number of arguments (three, four etc.). As a result, one arrives at an infinite set of coupled equations for the correlation functions of all orders which cannot be solved exactly. An approximation to handle this problem is to cut off this infinite hierarchy. Single densities can be calculated using the cluster approximation[19] well known in theory of phase transitions. The approximation is based on the relation

$$\rho^{(z+1)} = C_{\lambda} \prod_{i=1}^{z} c_{\mu_i}^{(\lambda)}(1). \tag{8}$$

In other words, the probability of finding a cluster of $(z+1)$ sites is approximated as a product of the probability C_{λ} to find the central site in the λ state and the conditional probabilities to find NN sites in the states $\mu_i = \sigma_i$ (its argument $r = 1$). From this general expression for the isolated particles one gets

$$C_{\lambda}^s = C_{\lambda}(c_0^{(\lambda)}(1))^z. \tag{9}$$

Since the conditional probabilities are limited from above [Eq. (6)], as expected the relation $C_{\lambda}^s \leq C_{\lambda}$ holds (not all particles are isolated). It will be shown below that by incorporation of particle attraction ($E_{\lambda\lambda} < 0$) this nonequality can be strengthened, $C_{\lambda}^s \ll C_{\lambda}$, due to formation of dimers, tri-

mers, and higher configurations. Similar to Eq. (2) the dimensional density of isolated particles can be found as

$$n_{\lambda}^{(1)} = \frac{C_{\lambda}^s}{a_0^3}. \tag{10}$$

4. The density of dimer particles

In the dimer configuration, the two NN particles are characterized by the lattice vectors $\mathbf{r}_l$ and $\mathbf{r}_m$ and the states $\lambda = \nu = A, B$, whereas all surrounding sites are empty. Such a state is described by the $(2z)$-point probability $\rho^{(2z)}$ provided that the states of the central sites are $\sigma_l = \sigma_n = \lambda$, whereas those of $(z-1)$ NN sites (surrounding each of the two central sites) are $\{\sigma\}_l^{z-1} = \{\sigma_1, \ldots, \sigma_{z-1}\} = \{0, \ldots, 0\}$, $\{\sigma\}_n^{z-1} = \{\sigma_1', \ldots, \sigma_{z-1}'\} = \{0, \ldots, 0\}$, respectively. Note that this is true for cubic lattices only (see Refs. 15,16). However, our formalism can be generalized for any lattice structures.

Using the cluster approximation, Eq. (8), we arrive at

$$\rho^{(2z)} = C_{\lambda} C_{\nu} F_{\lambda\nu}(1) \prod_{i=1}^{z-1} c_{\mu_i}^{(\lambda)}(1) \prod_{j=1}^{z-1} c_{\mu_j}^{(\nu)}(1). \tag{11}$$

Taking into account Eq. (11) and all possible spatial orientations of the dimer (a dumbbell), one gets

$$C_{\lambda}^d = \frac{z}{2} C_{\lambda}^2 F_{\lambda\lambda}(1)(c_0^{(\lambda)}(1))^{2(z-1)}. \tag{12}$$

The density of dimers is defined in such a way that the dimensional concentration $n_{\lambda}^{(2)} = C_{\lambda}^d/a_0^3$ gives a mean number of dimers per unit volume.

5. The mean particle number and aggregate size

In a similar manner the density of trimers, tetramers, and larger aggregates can be found. However, large aggregates (colloids) can be better characterized by such averaged quantities as aggregate size R_{λ} and the mean number of particles inside it, N_{λ}. For this purpose we can use the following arguments. By definition, $c_{\lambda}^{(\lambda)}(\mathbf{r})$ is the mean density of particles λ at the distance $\mathbf{r}$ from the central site occupied by a similar particle λ. If the particle distribution is random, $F_{\lambda\mu}(\mathbf{r}) = 1$, the local density coincides with the macroscopic one, $c_{\lambda}^{(\lambda)}(\mathbf{r}) = C_{\lambda}$. However, this is only the case if there are no particle interactions or reaction. In the general case the relations $F_{\lambda\mu}(\mathbf{r}) \to 1$ and $c_{\lambda}^{(\lambda)}(\mathbf{r}) = C_{\lambda}$ hold only asymptotically, as $r \to \infty$. This is why the quantity $\delta c_{\lambda}^{(\lambda)}(\mathbf{r}) = C_{\lambda}[F_{\lambda\lambda}(\mathbf{r}) - 1]$ gives the surplus particle density at short relative distances as compared to their random distribution. Its positive magnitude characterizes the aggregation of particles. Using $\delta c_{\lambda}^{(\lambda)}(\mathbf{r})$ as a weighting function, we can define the mean number of particles inside the aggregate as

$$N_{\lambda} = 1 + \sum_{\mathbf{r}} \delta c_{\lambda}^{(\lambda)}(\mathbf{r}) \tag{13}$$

and its radius

$$R_{\lambda} = \frac{1}{N_{\lambda}} \sum_{\mathbf{r}} |\mathbf{r}| \delta c_{\lambda}^{(\lambda)}(\mathbf{r}). \tag{14}$$

The unity on the right-hand side of Eq. (13) corresponds to the central particle in whose surroundings the excess particle density is integrated. For a random particle distribution, $F_{\lambda\mu}(\mathbf{r}) = 1$, and the definitions (13) and (14) yield $N_\lambda = 1$ and $R_\lambda = 0$, i.e., the concentration of dimers, trimers, etc. which always statistically exist, is assumed to be much smaller than the aggregation effect driven by the reaction and particle interaction. It should be noted here that in real experiments in insulating crystals concentrations of isolated centers, dimers, and trimers [the so-called F, F_2 (M), F_3 (R) centers], i.e., the smallest aggregates, on the one hand, and the large colloid size and a total concentration of metal (fraction of sites occupied by defects), on the other hand, can be estimated from absorption measurements.[5] Information about H aggregates is much less accurate, only the smallest H clusters are detectable by Raman spectroscopy. Gas bubble formation in irradiated CaF_2 has been reported in Ref. 20. In metals experimental information on the defect aggregation is even more qualitative.

IV. TRANSITION RATES

After definition of the spectrum of the site state variables $\sigma_l = \lambda$ the stochastic lattice Markovian model of the aggregation kinetics needs also the definition of the transition rates. The latter are monomolecular and bimolecular transitions.

A. Monomolecular transitions

The simplest, monomolecular transitions depend only on a single lattice site state whereas the states of surrounding sites remain unchanged. These transitions can be presented as

$$\sigma_l \overset{k}{\to} \sigma_l' \quad \text{or} \quad \lambda \overset{k}{\to} \lambda', \tag{15}$$

where the transition rate $k = P(\lambda \to \lambda')$ does not depend on the lattice vector $\mathbf{r}_l$. Examples are A (B) particle (defect) creation in an empty lattice site, $0 \to A$ and $0 \to B$, respectively.

$$P(0 \to A) = P(0 \to B) = p_0 = p a_0^3, \tag{16}$$

where p is defined in Sec. III as the irradiation intensity (dose rate). That is, Frenkel defects are created in pairs, each occupying two lattice sites. Depending on the irradiation conditions, the distance within such a pair can vary. Under an electron irradiation considered here it is known to be quite large, so that dissimilar defect creation can be considered as a random, uncorrelated creation of A and B particles in equal concentrations.[14,15] In principle, the spatial correlation of Frenkel defect pairs, AB, can also be taken into account[15] but it is not directly related to the problem of aggregation kinetics.

B. Bimolecular transitions

Such transitions are related to a simultaneous change of the state of two NN sites with lattice vectors $\mathbf{r}_l$ and $\mathbf{r}_n$. In the general case bimolecular transitions are described by the equation

$$\sigma_l \sigma_n \overset{k}{\to} \sigma_l' \sigma_n' \quad \text{or} \quad \lambda \nu \overset{k}{\to} \lambda' \nu'. \tag{17}$$

It is convenient to present the transition rate k taking into account the coordination number z: $k = K(\lambda \nu \to \lambda' \nu')/z$. Examples are: (i) dissimilar particle recombination,

$$AB \overset{k}{\to} 00 \quad \text{with} \quad K(AB \to 00) = \Omega, \tag{18}$$

(ii) particle diffusion (particle random walks on the lattice, $\lambda = A, B$),

$$\lambda 0 \overset{k}{\to} 0\lambda \quad \text{with} \quad K(\lambda 0 \to 0\lambda) = D_\lambda^0. \tag{19}$$

For simplicity we assume the recombination rate to be infinite, $\Omega \to \infty$, which corresponds to the instant recombination of defects with a restoration of the perfect lattice. The hop rates D_A^0 and D_B^0 have simple relations to the diffusion coefficients

$$D_\lambda = \frac{a_0^2}{z} D_\lambda^0, \quad D_\lambda = d_\lambda \exp\left(-\frac{E_\lambda}{k_B T}\right), \tag{20}$$

where d_λ is the diffusion prefactor and a_0 is the hopping distance (assumed to be equal to the lattice constant).

C. Energetic interaction of particles

Equations (17), (18), and (19) describe particle creation, diffusion, and recombination but neglect their energetic interaction. Due to this interaction the transition rate can depend on the NN states and temperature. Examples of such interactions are Coulomb and elastic attraction of defects in solids.[15,17,18] To take this into account, the monomolecular transition rate $P(\lambda \to \lambda')$ should be replaced by $\mathbf{P}(\lambda \to \lambda' | \{\sigma\}_l^z)$ and the bimolecular rate $K(\lambda \nu \to \lambda' \nu')$ by $\mathbf{K}(\lambda \nu \to \lambda' \nu' | \{\sigma\}_l^{z-1} \{\sigma\}_n^{z-1})$. This dependence can be found from the asymptotic behavior of the steady state of the kinetic system under study and the equilibrium Gibbs distribution. This problem arose in the study of the kinetic Ising model in lattice phase transitions. We follow here the general approach developed by us for the stochastic surface reactions.[16] The so-called *standard model* presented there allows us to obtain uniquely the rates of mono- and bimolecular transitions including the particle interactions. It should be stressed once more that we restrict ourselves to NN interaction. Due to the interaction similar particles begin to aggregate. It is clear that the probability of some particle in the center of an aggregate to find an empty NN site for a diffusion hop is quite small. Also, the hop probability for a particle at the periphery of the aggregate to leave it is because of the particle attraction smaller than the probability to hop into the interior of the aggregate and make it denser. This is why the aggregation kinetics should depend on temperature and the three interaction energies between similar and dissimilar particles, E_{AA}, E_{AB}, E_{BB}. For more details see Secs. VII and VIII and Eqs. (12)–(31) in Ref. 16.

A system of interacting particles can be characterized by the effective diffusion coefficient D_λ^{eff}. By definition, Eq. (19), rates of bimolecular hops are proportional to the diffusion coefficients. Let us define the effective dimensional diffusion coefficient, $D_\lambda^{\text{eff}}/D_\lambda$. Here D_λ is the usual diffusion coefficient in a dilute system consisting of ν isolated defects

which is proportional to the rate $K(\lambda 0 \to 0\lambda)$. In turn, in the dense system of interacting particles D_λ^{eff} is proportional to the avaraged transition rate $\langle \mathbf{K}(\lambda 0 \to 0\lambda | \{\sigma\}_l^{z-1} \{\sigma\}_n^{z-1}) \rangle$. The latter transition rate is averaged $(\langle \dots \rangle)$ over all configurations of particles surrounding a given particle. This can be done using the cluster probability, Eq. (11). As we show below in Sec. VI D, under particle aggregation the parameter $D_\lambda^{\text{eff}}/D_\lambda$ is by many orders of magnitude less than unity thus characterizing migration properties in a dense interacting system.

V. MASTER EQUATIONS

As was noted above, the stochastic Markovian process is uniquely defined by a set of mono- and bimolecular transition rates. The relevant, discrete-lattice formalism based on the hierarchy of the correlation functions has been presented recently[15,16] and illustrated by the particle aggregation in the course of the catalytic surface reaction $A + \frac{1}{2}B_2 \to 0$. This is why in this paper we do not repeat complicated general equations which can be solved only using special iterative procedures. In contrast, we discuss only the basic idea of the approach and its application to the particular bulk $A + B \to 0$ reaction in three dimensions. In fact, the latter reaction under study is mathematically isomorphic to the above-mentioned surface catalytic reaction where the molecule adsorption/desorption is replaced by the defect production rate p in the bulk.

The final set of kinetic equations read

$$\frac{dC_\lambda}{dt} = G_\lambda(C,F),\qquad (21)$$

$$\frac{dF_{\lambda\mu}(\mathbf{r})}{dt} = G_{\lambda\mu}(C,F),\qquad (22)$$

where G_λ and $G_{\lambda\mu}$ are expressions nonlinear in the lattice densities and the correlation functions. They arise due to the systematic use of approximations such as the cluster approximation, Eq. (11) (for more details see Ref. 16). To illustrate this approach, we write down the structure of Eq. (21) where

$$G_\lambda = G_\lambda^{\text{in}} - G_\lambda^{\text{out}},\qquad (23)$$

$$G_\lambda^{\text{in}} = \sum_{\lambda'} P'(\lambda' \to \lambda) C_{\lambda'} + \sum_{\lambda'\nu'\nu} K'(\lambda'\nu'$$
$$\to \lambda\nu) F_{\lambda'\nu'}(1) C_{\lambda'} C_{\nu'},\qquad (24)$$

$$G_\lambda^{\text{out}} = \sum_{\lambda'} P'(\lambda \to \lambda') C_\lambda + \sum_{\lambda'\nu'\nu} K'(\lambda\nu$$
$$\to \lambda'\nu') F_{\lambda\nu}(1) C_\lambda C_\nu.\qquad (25)$$

The equations above describe all possible mono- and bimolecular processes. Formally these equations remind us of the usual rate equations for defect concentrations.[9] However, the key factor is that the functions $P'(\lambda \to \lambda')$ and $K'(\lambda\nu \to \lambda'\nu')$ are *effective* transition rates. These quantities are obtained via averaging over the nearest-neighbor states based
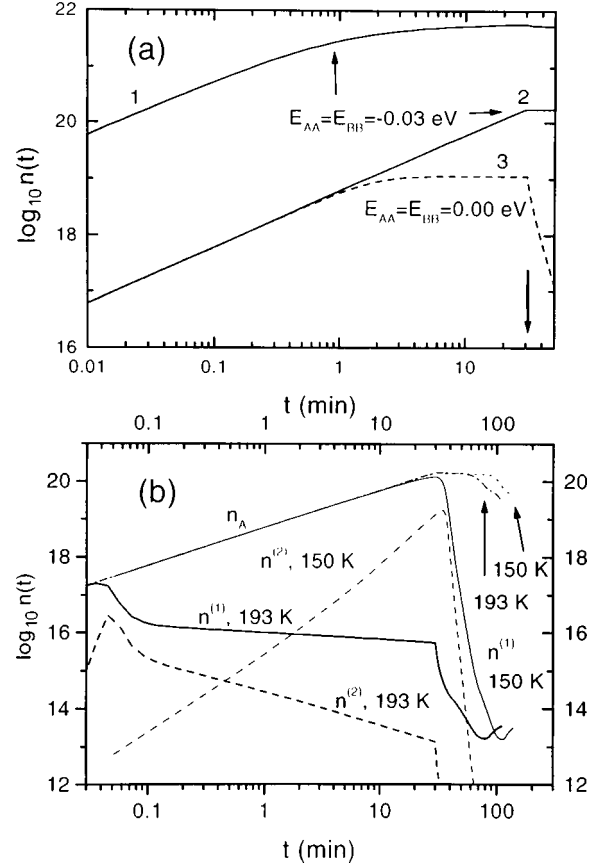

FIG. 1. (a) Time development of total F, H concentrations (in cm^{-3}) under irradiation at 193 K for 30 min (shown by an arrow) with a subsequent heating at the rate 1.3 K/min. Curves 1 and 2 show the effect of the dose rate ($p = 10^{20}$ and $p = 10^{17}$ cm^{-3} s^{-1}, respectively), whereas curve 3 shows the effect of the neglect in the latter case of similar defect interation $E_{\lambda\lambda} = 0$, $\lambda = A,B$. Note rapid defect recombination in case 3 when irradiation is switched off. (b) The dynamics of single, $n^{(1)}$, and dimer, $n^{(2)}$, H center aggregation and total H concentrations, n_A, for a dose rate $p = 10^{17}$ cm^{-3} s^{-1} under irradiation at 193 K (as in curve 2 above) and at 150 K.

on the statistical weights: Eq. (8) for the calculation of quantity (26) and Eq. (11) for the quantity (27) below:

$$P'(\lambda \to \lambda') = \langle \mathbf{P}(\lambda \to \lambda' | \{\sigma\}_l^z) \rangle,\qquad (26)$$

$$K'(\lambda\nu \to \lambda'\nu') = \langle \mathbf{K}(\lambda\nu \to \lambda'\nu' | \{\sigma\}_l^{z-1} \{\sigma\}_n^{z-1}) \rangle.\qquad (27)$$

The lengthy expressions for these functions are given in the Appendix of Ref. 16 and consist of 35 equations. As a result, the kinetic equations depend on the kinetic constants, temperature and NN interaction energies. The particle aggregation is characterized by the shape of the joint correlation functions; at distances $\mathbf{r} = |\mathbf{r}_l - \mathbf{r}_m|$, where some joint density considerably exceeds the asymptotic value of unity, a large excess of neighboring similar particles (i.e., an aggregate) is found compared to the random (Poisson) distribution. The aggregate size can be estimated as the distance at which the joint correlation functions $F_{\lambda\lambda}(\mathbf{r})$ approach the value of unity. Our stochastic formalism operates with a finite set of lattice densities C_λ and joint correlation functions $F_{\lambda\mu}(\mathbf{r})$.
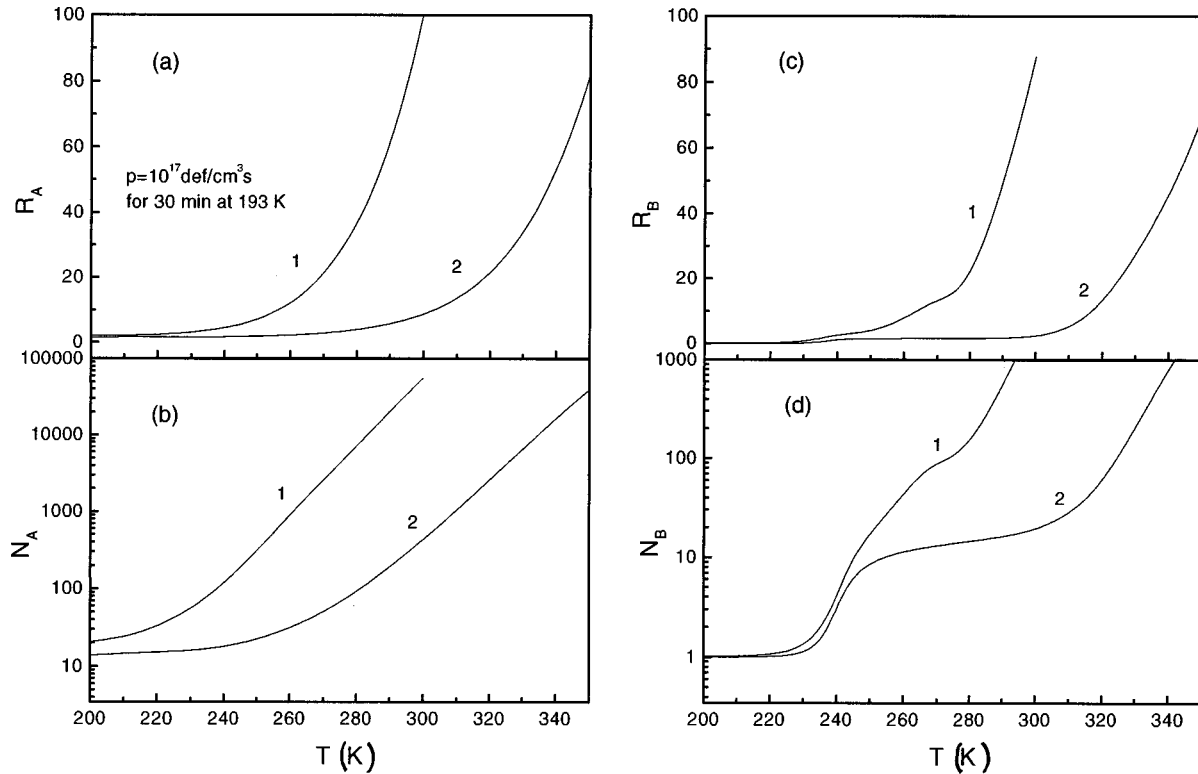
FIG. 2. (a) Heating-induced growth of the mean radius of H aggregates, R_A (in units of the $F-F$ distance, $a_0=2.73$ Å in CaF$_2$). Note that H and F defects are denoted as defects A and B, respectively. (b) The mean number of particles inside each aggregate, N_A. Irradiation with the dose rate $p=10^{17}$ cm^{-3} s^{-1} for 30 min. Curves 1 and 2 correspond to the attraction energies $E_{AA}=E_{BB}=-0.02$eV. and -0.03 eV, respectively; (c) and (d) the same for the F centers, respectively.

The set of resulting ordinary differential equations to be calculated is formally infinite due to the infinite number of lattice sites $\mathbf{r}_l$ and $\mathbf{r}_m$; but in practice we restrict ourselves to finite relative distances (correlation lengths) which is justified by the short-range nature of the spatial correlations in the particle densities.

The relevant computer code KINETIKA (Ref. 21) permits us to calculate the time development of the total defect concentrations, single and dimer centers, effective diffusion coefficients and reaction rate, mean sizes of the aggregates, and the number of particles therein. This gives a complete picture of the diffusion-controlled aggregation process.

VI. RESULTS FOR CaF$_2$

The key parameters which govern particle aggregation in a binary system (Frenkel defects A and B discussed above) include: (i) the lattice parameter a_0 which usually serves also as the recombination radius. (ii) The activation energies for diffusion hops E_λ and pre-exponential factors d_λ ($\lambda = A, B$) which define the diffusion coefficient for the isolated particles A and B. The activation energies for interstitials and vacancies may differ by an order of magnitude (e.g, $E_A = 0.1$ eV and $E_B = 1$ eV in NaCl). (iii) similar and dissimilar particle interaction energies E_{AA}, E_{AB}, and E_{BB}. These energies, along with the temperature, directly control the rate of the H, F center attachment and detachment to/from the aggregate of similar particles. These three intrinsic parameters characterize the actual physical system, whereas the remaining two parameters describe the external condi-

tions: (iv) the temperature T, and (v) the dose rate p characterizing the irradiation intensity. In the particular case of CaF$_2$ the activation energies for the F and H center diffusion are known from the thermostimulated luminescence experiments (0.7 and 0.46 eV, respectively).[22] The energies of the elastic interactions are less well known. Calculations for pairs of NN defects in KBr show that they are about -0.02 to -0.05 eV.[23] In this paper we vary these energies in the mentioned limits and compare results with experimental data. For simplicity the defect interaction energies are assumed to be equal, $E_{AA} = E_{BB}$. Additional calculations have demonstrated that for unequal interaction energies results remain qualitatively the same. It is also assumed that there is no attraction between H and F centers; an inclusion of their attraction only slightly accelerates the recombination rate.

To make the model as simple as possible, we assume that parameters of a dense defect system are entirely determined by parameters of isolated single particles or isolated pair particles. This is true for NN interactions between particles treated in this paper. Effects of long-range particle interaction are not considered here, this is a subject of another study which is in progress now. Note however, that the effective parameters for dense systems, such as the diffusion coefficients of particles to be discussed below, can in the framework of our simple model differ by many orders of magnitude from properties of isolated particles. This justifies the use of a simple (and thus, handable) model for colloid formation.

In real experiments samples are irradiated at a given fixed

temperature for a certain time, $t < t_0$, then the irradiation is switched off, and the sample is heated with a constant rate. We have modeled this process, asuming that after irradiation $T(t) = T_0 + \gamma(t - t_0)$, where γ is the heating rate (typically, 1–2 K/min). We compare our calculations with the Ca-colloid growth kinetics observed in Ref. 5 for CaF$_2$ irradiated by low-energy electrons at low ($T_0 \approx$ 200 K) temperatures and subsequently heated with the rate $\gamma = 1.3$ K/min. This irradiation corresponds to a dose rate of about $p = 10^{17}$ cm^{-3} s^{-1}.

A. Defect concentration growth under irradiation

Let us start with a study of the kinetics of defect concentration growth in CaF$_2$ under irradiation at low temperatures when the F centers are definitely immobile but the H centers are moving either slowly (150 K) or are already quite mobile (193 K). The first conclusion from curve 2 in Fig. 1(a) is that up to the end of the irradiation (shown by an arrow at the time scale) the defect concentration grows almost linearly with time. Under such a dose rate the concentration saturation can be expected after 2 h of irradiation. The magnitude of the defect concentration achieved agrees well with experimental data.[5]

Simulation of a very intensive irradiation (curve 1) indicates that the theoretical prediction of the defect concentration which can be achieved is of the order of 10^{22} cm^{-3}. Lastly, curve 3 clearly demonstrates that *neglect* of the defect interaction leads to a reduction by several orders of magnitude in defect concentrations at their saturation and a very fast recombination when irradiation is switched off.

The time development of the total H-aggregate concentration (n), and of single and dimer centers is illustrated in Fig. 1(b). Total concentrations of H centers almost coincide at the two temperatures; the H center concentration at 150 K irradiation exceeds that at 193 K irradiation only for $t > 70$ min when irradiation is switched off and a sample is heated up by about 50 K. It is seen that the concentration of single H centers, $n^{(1)}$, decreases due to growth of the dimer concentration, $n^{(2)}$, and the latter drops also at a certain time t_0 due to the growth of larger aggregates. The time t_0 decreases by three orders of magnitude when the irradiation temperature increases just from 150 K up to 193 K. For the value of $E_B = 0.7$ eV the F centers at temperatures shown in Fig. 1 are immobile and their aggregation occurs only on heating *after* irradiation.

B. Aggregate growth upon heating

Curves 1 in Figs. 2(a) and 2(c) corresponding to the defect attraction energies of -0.02 eV show that the H and F center aggregates' radii as well as the mean number of defects therein [Figs. 2(b) and 2(d), respectively] begin to grow synchronously, at 250 K when the F centers become mobile. (Note that the H centers are mobile already above 150 K.) Due to computational difficulties we cannot follow the last stage of the large aggregate growth but its typical size of 100 $a_0 = 28$ nm is close to the experimental value (25 nm). The experimentally observed temperature for a sharp metal colloid growth is 270 K. An increase of the interaction energy by 50% (curves 2) shifts the temperature of the efficient defect aggregation by about 50 K.
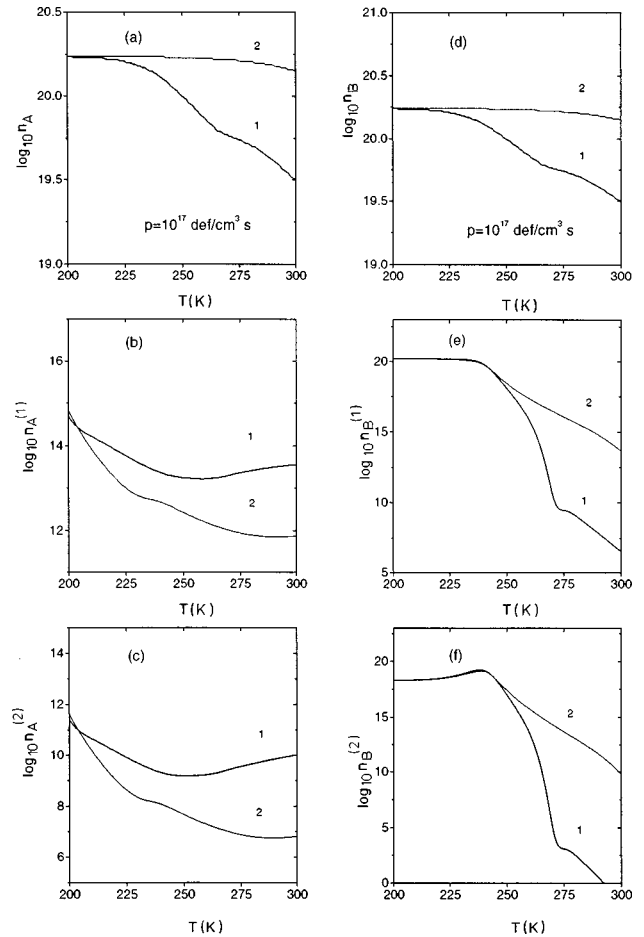

FIG. 3. Temperature development of the total H center concentration (a), that for single H centers (b) and dimer, H_2 center concentration (c). Curves 1 and 2 are for the interaction energies given in Fig. 2; (d)–(f)—the same for the F centers.

The dynamics of the total H center concentration as well as that for single centers and dimers is plotted in Figs. 3(a)–3(c) as a function of temperature. Since at 200 K the H centers already have aggregated, the concentration of single and dimer centers is smaller than the total H concentration by 5 and 8 orders of magnitude, respectively. [Note from Fig. 2(b) that such a small aggregate contains about 20 H centers.]

It follows from Figs. 3(d)–3(f) that at 200 K only single F centers exist in a concentration close to 10^{21} cm^{-3}, whereas the concentration of dimers is smaller by three orders of magnitude. As the temperature reaches the one where the F centers become mobile, 250 K, both concentrations drop by many orders of magnitude. However, the total F concentration decreases insignificantly after heating up to 350 K and exceeds 10^{19} cm^{-3} s^{-1}. This indicates that most of the F centers are gathered now into large aggregates and only a small fraction recombines with the H centers. This is another confirmation of what we concluded from an analysis of Fig. 2.

C. Reaction rate

The reason why the recombination becomes so inefficient is clear from Fig. 4. The reaction rate between H and F
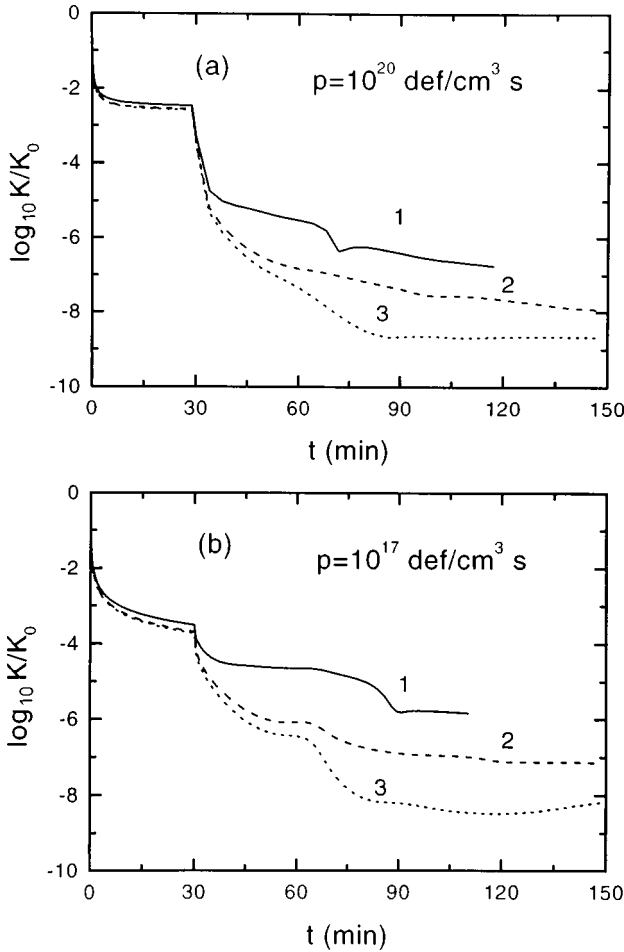
FIG. 4. (a) The dynamics of the dimensionless reaction rate K as a function of time. The dose rate is $p = 10^{20}$ cm^{-3} s^{-1} and the interaction energies -0.02, -0.03, and -0.04 eV (curves 1, 2, and 3, respectively). (b) The same for $p = 10^{17}$ cm^{-3} s^{-1}.

FIG. 5. Time development of the dimensionless effective diffusion coefficients for the H centers at the dose rates of $p = 10^{20}$ cm^{-3} s^{-1} (a) and $p = 10^{17}$ cm^{-3} s^{-1} (b). Parameters for curves 1, 2, and 3 are the same as in Fig. 4.

centers rapidly drops down at the very beginning of irradiation, by three orders of magnitude in about a minute. Its stabilized value does not depend on the interaction energy. This is caused by the H center aggregation shown above in Figs. 1 and 2. As a result, such H aggregates are rather immobile which prevents H and F recombination. The main contribution to the recombination comes from newly created H centers whose concentration is proportional to the dose rate p . This is why, when irradiation is switched off, the reaction rates are reduced additionally, by an order of magnitude for $p = 10^{17}$ cm^{-3} s^{-1} but by two orders of magnitude for $p = 10^{20}$ cm^{-3} s^{-1}. This reduction depends also on the defect interaction energy.

D. Defect mobility

The dynamics of the H center mobility for two dose rates is plotted in Figs. 5(a) and 5(b), respectively. These plots demonstrate a clear correlation between defect mobilities and recombination rate. Curve 1 in Fig. 5(a) shows that the H center mobility repeats a two-step fall and stabilization (plateau) observed for K in Fig. 4. What is interesting here is the fact that upon heating, the effective diffusion coefficient, D_A^{eff}, starting at a certain temperature begins to increase,
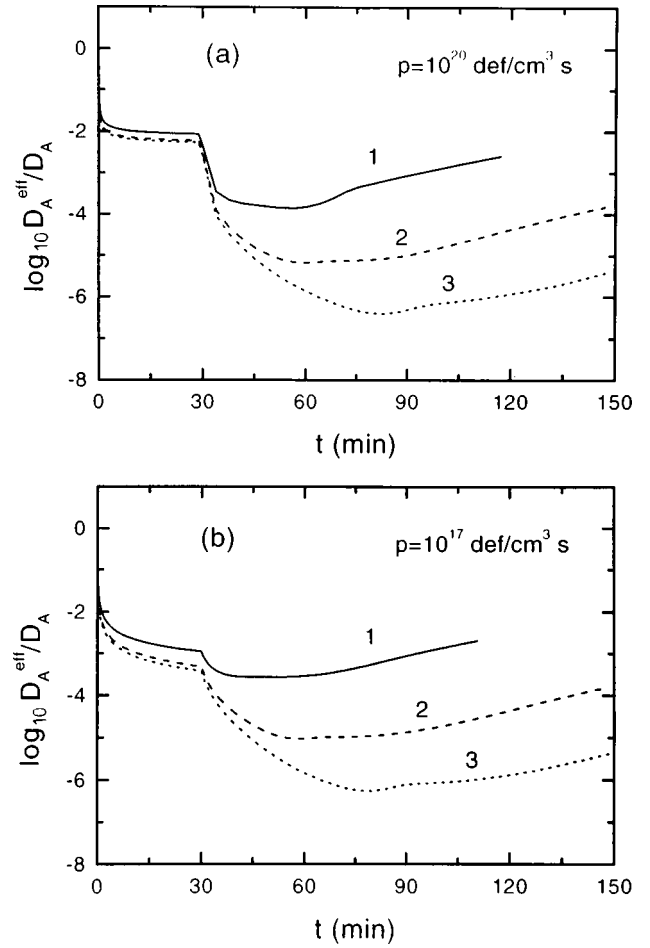
very likely because of the separation of some of H centers from their aggregates which leads to recombination of some of them with the F centers [note the concentration decay in Fig. 2(a)]. This recombination is an important factor for a subsequent considerable growth of the H center aggregates which takes place synchronously with the aggregation of the F centers, at $T \approx 250$ K. Recombination results in the disappearance of numerous dispersed F centers in a region around small H aggregates. This creates additional space necessary for further considerable growth of the H aggregates.

Unlike the H centers, the F centers remain immobile up to the time $t = 60$ min when the temperature approaches the F center mobility edge, 250 K [Fig. 6(a)]. Reduction in the F center mobility directly indicates their aggregation. Stabilization of the effective diffusion coefficient at $T \approx 300$–350 K (curves 1 to 3) arises due to formation of stable aggregates. The latter are in a dynamical equilibrium with the F centers joining and leaving the aggregate. This is why the stabilization plateau occurs at higher temperatures, as $E_{\lambda\lambda}$ increases from -0.02 to -0.04 eV.

Figure 6(b) demonstrates the effect of unequal interaction energies. A comparison of curves 1 in Figs. 6(a) and 6(b) shows that an increase of E_{AA} stimulates the F mobility.
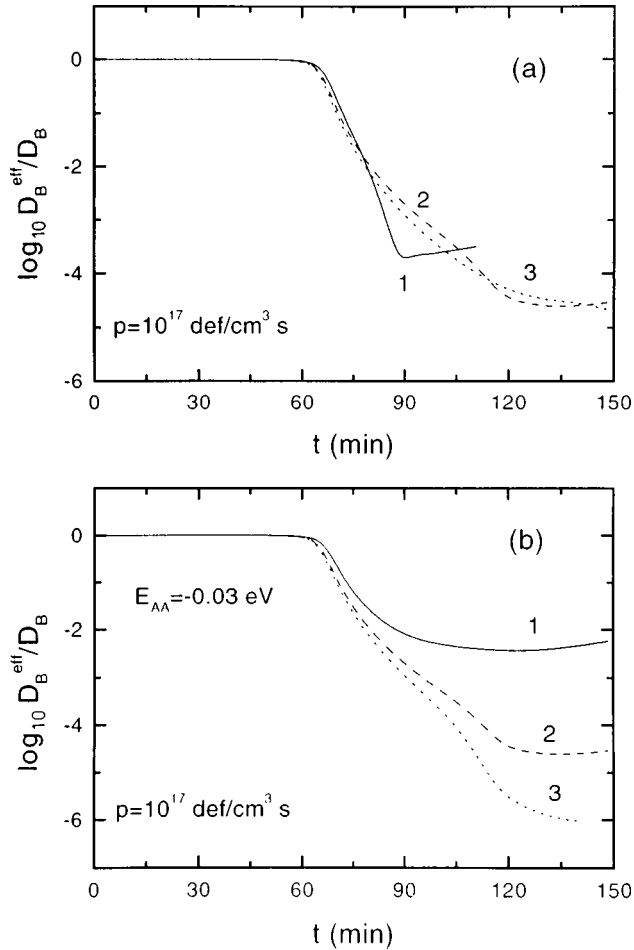
FIG. 6. (a) The same as in Fig. 5(b) for the F centers. (b) the effect of unequal interaction energies, $E_{AA}=-0.03$ eV is fixed; $E_{BB}=-0.02$, -0.03, and -0.04 eV (curves 1–3, respectively).

E. Spatial distribution of defects

It is interesting to compare the results given above with the irradiation at higher temperatures when both H and F centers are very mobile. To this end, we performed calculations for the irradiation at room temperature, 300 K. In agreement with experiment, the total concentration of F defects at the end of irradiation is nearly the same as for low-temperature irradiation. Unlike the previous study at 193 K, we observe now growth of the F aggregates *during* the irradiation. However, the mean radius of this aggregate remains small ($R_B < 10$ a_0 after 30 min) due to efficient F-H recombination. This is again in qualitative agreement with experiments where only nm-scale metal colloids are observed during irradiation.

As the irradiation is switched off, F aggregates begin to grow. This process is well illustrated by an analysis of the joint correlation functions characterizing the relative *spatial distribution of defects* (Fig. 7). Large values of the joint correlation functions of similar defects, F_{AA}, F_{BB} (note their logarithmic scale) at short relative distances r clearly demonstrate a strong aggregation of *both* H and F centers. At the end of the irradiation (plot a) we have a relative distance of $r \approx 10 a_0$ where F_{BB} (curve 2) approaches the asymptotic value of unity. This agrees with the above-mentioned calculation of the effective radius R_B. The effective radius of the
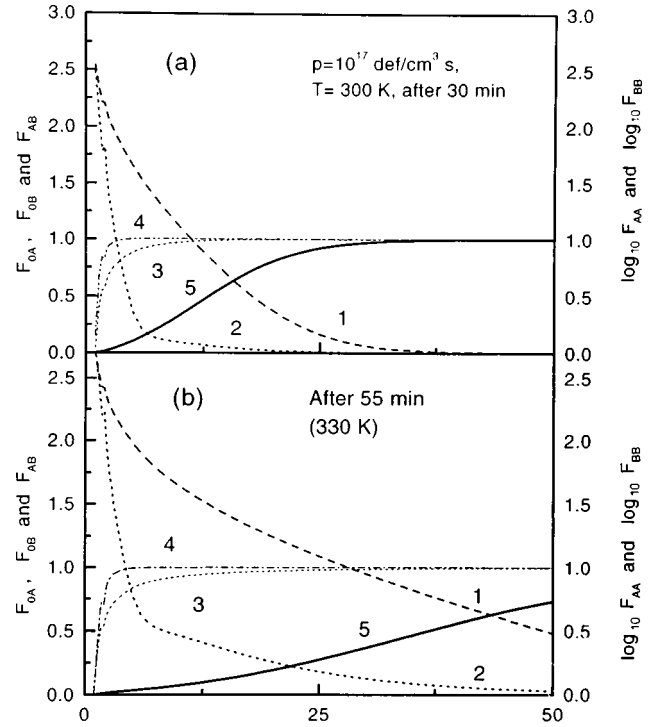

FIG. 7. The joint correlation functions vs the relative distance r between particles. Irradiation at 300 K, (a) corresponds to the end of irradiation, (b) after subsequent 25 min heating (up to 330 K). Curves 1 and 2 demonstrate the $H-H$ and $F-F$ center correlations, curve 3,4 ''empty site-F center'' and ''empty site-H center'' correlations, and curve 5 correlation of dissimilar defects ($F-H$). Note that F_{AA} and F_{BB} are plotted in the semilogarithmic scale.

H aggregates is larger, about 30 a_0. After 25 min of heating (plot b) the radii of F and H aggregates increase to $R_B \approx 30$ a_0 and $R_A \approx 70$ a_0, respectively. The correlation function for dissimilar defects, $F_{AB}(r)$, (curve 5) is anticorrelated to F_{AA} and F_{BB}. At the end of the irradiation it increases from zero at $r \leqslant a_0$ up to unity at $r \approx 30$ a_0, which gives us an estimate of the average distance *between* H and F aggregates.

Lastly, the joint correlation functions of an empty site with a defect, F_{0A} and F_{0B}, curves 3 and 4, show that these aggregates have small, dense cores (there are almost no empty sites in their centers but they are quite loose on their periphery, $r \geqslant 10$ a_0).

VII. DISCUSSION AND CONCLUSIONS

The microscopic theory of diffusion-controlled radiation defect aggregation reproduces the main experimental results for the electron-irradiated CaF_2 and permits us to understand the mechanism and kinetics of this process. Despite the fact that the H and F centers have very different mobilities, and start to perform diffusion hops at 150 and 250 K, respectively, they show *simultaneous* aggregation. The growth of large aggregates is also determined by the defect interaction energy. Thus, curve 2 in Fig. 2(d) shows that after formation at 250 K of small aggregates of F centers (about 10 defects in each) they do not grow further until the temperature in-

creases up to 320 K. At this temperature the thermal energy, $k_B T$, turns out to be close to the interaction energy, E_{BB}, and single F centers start to leave small aggregates which is a precondition for growth of large aggregates. Such a process of the transformation of small aggregates into large ones is often called *Ostwald ripening*. Note that we present here the first microscopic theory for this process; previous phenomenological theories are unable to incorporate the defect interactions (see Ref. 24 and references therein). Even our simplifed treatment of defect interaction required a lot of computational time (typically, several days or a week). This is why it is hard to go beyond the NN approximation for defect interaction.

The scenario of this cooperative process can be summarized as follows. Under irradiation mobile H centers aggregate first (at $t \approx 10^{-3} s$) forming small clusters (typically of 10 defects) whereas F centers remain randomly distributed. As irradiation continues, the size of these (practically immobile) H clusters does not change with time, only their number increases. After irradiation upon heating to some critical temperature T_c, H centers begin to detach from small aggre-

gates (provided $k_B T_c \approx E_{AA}$). This results in single H center recombination with the nearby F centers and the appearance of a region around H clusters free of F centers. This process leads to the transformation of small H clusters into large ones (with the average number of defects $N_A \approx 10^5$).

At the temperature when the F centers start to move, they form, first of all, small clusters, very similarly to those of H centers created at short times. Similarly to the H aggregation, their subsequent rearrangment into large aggregates takes place at the temperature T_0 when $k_B T_0 \approx E_{BB}$. If $E_{AA} \approx E_{BB}$, aggregation of both kinds of defect occurs simultaneously.

*Electronic address: kuzovkov@latnet.lv

[1] A.E. Hughes and S.C. Jain, Adv. Phys. **28**, 717 (1979); P.W. Levy, J. Phys. Chem. Solids **52**, 319 (1991); W.J. Soppe and J. Prij, Nucl. Technol. **107**, 243 (1994).

[2] M. Zaiser, W. Frank, and A. Seeger, Solid State Phenom. **23/24**, 203 (1992); P. Bellon and G. Martin, *ibid.* **30/31**, 107 (1993).

[3] E.R. Hodgson, A. Delgado, and J.L. Alvarez Rivas, Phys. Rev. B **18**, 2911 (1978); J.R.W. Weerkamp, J.C. Groote, J. Seinen, and H.W. den Hartog, *ibid.* **50**, 9781 (1994); J. Seinen, J.C. Groote, J.R.W. Weerkamp, and H.W. den Hartog, *ibid.* **50**, 9787 (1994); J. Seinen, J.R.W. Weerkamp, J.C. Groote, and H.W. den Hartog, *ibid.* **50**, 9793 (1994); J.C. Groote, J.R.W. Weerkamp, J. Seinen, and H.W. den Hartog, *ibid.* **50**, 9798 (1994); H.W. den Hartog, J.C. Groote, and J.R. Weerkamp, Radiat. Eff. Defects Solids **139**, 1 (1996).

[4] A.T. Davidson *et al.*, J. Phys. Condens. Matter **7**, 32 11 (1995).

[5] R. Bennewitz, C. Günther, M. Reichling, E. Matthias, R.M. Wilson, and R.T. Williams, Radiat. Eff. Defects Solids **137**, 19 (1995); E. Stenzel, N. Bouchaala, S. Gogol, T. Klotzbücher, M. Reichling, and E. Matthias, Mater. Sci. Forum **239-241**, 591 (1997); R. Bennewitz, C. Günther, M. Reichling, E. Matthias, S. Vijayalakshmi, A.V. Barnes, and N.H. Tolk, Appl. Phys. Lett. **66**, 320 (1995); N. Bouchaala, Ph.D. thesis, Freie Universität Berlin, 1997.

[6] V.M. Orera and E. Alacala, Phys. Status Solidi A **44**, 717 (1977); W.J. Weber, G.J. Exarhos, and L.M. Wang, in *Microstructure of Irradiated Materials,* edited by I.M. Robertson *et al.*, MRS Symposia Proceedings No. 373 (Materials Research Society, Pittsburgh, 1995), p. 311.

[7] S.J. Zinkle, Nucl. Instrum. Methods Phys. Res. B **91**, 234 (1994).

[8] M. C. Cross and P.C. Hohenberg, Rev. Mod. Phys. **65**, 851 (1993).

[9] W.J. Soppe, J. Phys. Condens. Matter **5**, 3519 (1993).

[10] U. Jain, Ph.D. thesis, Harwell University, 1977; U. Jain and A.B. Lidiard, Philos. Mag. **35**, 245 (1977); A.B. Lidiard, Philos. Mag. A **39**, 647 (1979).

[11] E.A. Kotomin, M. Zaiser, and W.J. Soppe, Philos. Mag. A **70**, 313 (1994).

[12] V.N. Kuzovkov and E.A. Kotomin, Phys. Scr. **47**, 583 (1993); **50**, 720 (1994).

[13] V.N. Kuzovkov and E.A. Kotomin, J. Phys. Condens. Matter **7**, L481 (1995).

[14] V.N. Kuzovkov and E.A. Kotomin, Rep. Prog. Phys. **51**, 1479 (1988); E.A. Kotomin and V.N. Kuzovkov, *ibid.* **55**, 2079 (1992).

[15] E.A. Kotomin and V.N. Kuzovkov, *Modern Aspects of Diffusion-Controlled Reactions* (Cooperative Phenomena in Bimolecular Processes), Compehensive Chemical Kinetics Vol. 34 (Elsevier, Amsterdam, 1996).

[16] J. Mai, V.N. Kuzovkov, and W. von Niessen, J. Phys. A **29**, 6205 (1996); **29**, 6219 (1996).

[17] V.N. Kuzovkov and E.A. Kotomin, J. Chem. Phys. **98**, 9107 (1993); J. Stat. Phys. **72**, 127 (1993).

[18] I.M. Sokolov and A. Blumen, Phys. Rev. E **50**, 2335 (1994).

[19] H. Mamada and F. Takano, J. Phys. Soc. Jpn. **25**, 675 (1968).

[20] R. Zanetti, A.L. Bleloch, M.P. Grimshaw, and G.A.C. Jones, Philos. Mag. Lett. **69**, 285 (1994).

[21] V.N. Kuzovkov (unpublished).

[22] K. Atobe, J. Chem. Phys. **71**, 2588 (1979).

[23] K. Bachmann and H. Peisl, J. Phys. Chem. Solids **31**, 1525 (1970).

[24] L.A. Maksimov, A.I. Ryazanov, K.-H. Heinig, and S. Reiss, Phys. Lett. A **213**, 73 (1996); S.A. Kukushkin and V.V. Slyozov, J. Phys. Chem. Solids **57**, 195 (1996); J.A.D. Wattis and P.V. Coveney, J. Chem. Phys. **106**, 9122 (1997).